DOI: 10.26599/FSHW.2026.9251076

Contents lists available at SciOpen

Food Science and Human Wellness

journal homepage: https://www.sciopen.com/journal/2097-0765

China Food Publishing Co.

Protective Effects of Praeparatus *Gardenia Fructus* Oil and Its Active Constituents Against Oxidative Neurodegeneration: Evidence from *In Vitro* and *In Vivo* Studies

Qinxue Ni[a,b,1,*], Yuanyuan Chen[a,1], Zhengxuan Jiao[c,d,1], Lin Chen[e], Yanming Ren[a], Youzuo Zhang[a,b], Kang Chen[c,d,*]

[a] *Zhejiang Provincial Key Laboratory of Resources Protection and Innovation of Traditional Chinese Medicine, College of Food and Health, Zhejiang A & F University, Linan 311300, China*

[b] *Zhejiang Jiaozhi Technology Co., Ltd, Hangzhou, Zhejiang 310021, China*

[c] *College of Food Science and Engineering, Ningbo University, Ningbo 315211, China*

[d] *Institute of Sericultural and Tea, Zhejiang Academy of Agricultural Sciences, Hangzhou, Zhejiang 310021, China*

[e] *Institute of One Health Science, School of Civil & Environmental Engineering and Geography Science, State Key Laboratory for Quality and Safety of Agro-products, Ningbo University, Ningbo 315211, China*

[f] *International Science and Technology Cooperation Base for Coastal Agricultural Water Resilience and One Health of Zhejiang Province, Ningbo 315211, China*

ABSTRACT: Neurodegenerative disorders demand safe, multi-targeted interventions. We revealed praeparatus *Gardenia Fructus* oil (PGFO) as a novel neuroprotective functional oil, outperforming raw and stir-baked *Gardenia Fructus* oil, as well as conventional edible oils. In H_2O_2-injured PC12 cells, PGFO restored redox balance and enhanced antioxidant enzymes, with effects stronger than those of isolated fractions, suggesting synergistic bioavailability within the oil matrix. Transcriptomics indicated modulation of the neuroactive ligand-receptor interaction and tryptophan pathways might be involved in its protective mechanism. In APP/PS1 mice, PGFO improved cognition, preserved neuronal integrity, reduced oxidative stress and neuroinflammation, and reshaped gut microbiota with elevated short-chain fatty acids. The study provides a theoretical basis for the development of PGFO as a neuroprotective dietary ingredient. These findings establish PGFO as a prototype functional oil integrating lipid-based delivery, neuromodulation, and gut–brain signaling, providing a promising dietary strategy against Alzheimer's disease.

Keywords: *Gardenia Fructus* oil; PC12 cells; neuroprotective; neuroactive ligand-receptor interaction pathway; tryptophan metabolism pathway; bioavailability

1. Introduction

Neurodegenerative diseases—such as Alzheimer's, Parkinson's, and Huntington's—are age-related disorders marked by progressive loss of cognitive and motor function[1]. Although their etiology involves

[1] These authors contributed equally to this work.
***Corresponding author**
niqinxue@zafu.edu.cn; chenkang@nbu.edu.cn

Received 30 November 2025
Received in revised from 25 January 2026
Accepted 24 February 2026

multiple mechanisms, notably oxidative stress and neuroinflammation[2], effective long-term therapies remain elusive. The chronic nature of these disorders imposes a heavy burden on patients, families, and healthcare systems[3]. Additionally, side effects and clinical manifestations of long-term medication drive interest in natural bioactive and dietary approaches for prevention and mitigation.

Given the central role of oxidative stress and neuroinflammation in neurodegenerative diseases such as Alzheimer's disease, it is particularly important to find safe and long-term dietary intervention plans. In recent years, dietary phytochemicals have shown broad prospects in this field due to their multi-target properties[4]. In this context, this study focuses on the medicinal and edible resource Gardenia jasminoides, aiming to explore the neuroprotective effects of its processed oil.

Gardenia Fructus (GF; “Zhizi”), the dried ripe fruit of Gardenia jasminoides Ellis, which is listed in the Chinese pharmacopeia, has been used for centuries in traditional Chinese medicine to treat anxiety, jaundice, liver disorders, and fever. Several studies have shown its efficacy against central nervous system disorders, including insomnia, depression, cognitive decline, Alzheimer’s and Parkinson’s diseases, due to its rich profile of iridoids, crocins, flavonoids and phenolic acids, which exhibit antioxidant, anti-inflammatory and anti-apoptotic effect[5-9]. Among GF’s constituents, geniposide and crocetin are recognized as primary neuroprotective agents[10, 11]. In the Chinese Pharmacopoeia, GF is classified into four forms—raw, stir-baked, praeparatus, and carbonized—according to increasing roasting temperatures. Processing not only alters its physical appearance but also its phytochemical profile and therapeutic efficacy: notably, praeparatus GF (roasted at intermediate temperatures) contains higher levels of crocetin and demonstrates superior antioxidant and anti-inflammatory activities compared to both raw (here refers to GF only subjected to steaming inactivation at 120℃ for 20–30 min followed by sun-drying, without any subsequent roasting treatment; the term “raw” reflects its lack of roasting rather than no processing) and stir-baked (a mild roasting process: GF is heated in a rotating stainless-steel drum at 150℃ for 25 min, with continuous stirring to ensure uniform heating) GF[12-15].

Since 2003, GF has been classified by China’s Ministry of Health as a dual-use resource for both food and medicine. Its oil (GFO) is valued for abundant unsaturated fatty acids and phytochemicals[16-18]. GFO has shown hepatoprotective effects in liver injury[19], to improve estradiol levels and bone density *via* COX-2 upregulation[20], and to demonstrate central-nervous-system benefits[21-23]. However, despite these , critical questions remain unanswered. First, the impact of different processing methods (raw, stir-baked, or praeparatus GFO) on the neuroprotective efficacy of GFO itself has not been systematically evaluated. Second, it is unknown whether the bioactivity of GFO results from a synergistic interplay of its components within the intact oil matrix, rather than from the action of isolated fractions. Third, the mechanistic pathways through which GFO confers neuroprotection remain poorly understood, especially regarding its possible interaction with the gut–brain axis.

In this study, we test the hypotheses that PGFO confers superior neuroprotection due to its higher phenolic content; that the intact oil matrix is required for maximal efficacy, potentially by enhancing

bioavailability and constituent synergy; and that its benefits involve not only antioxidant effects but also modulation of neuroactive pathways and the gut–brain axis, supporting provide a substantive scientific basis for considering PGFO as a promising functional edible oil for the dietary support of brain health and the prevention of neurodegenerative disorders.

2. Materials and Methods

2.1 Preparation of GF Oil Samples

Raw *Gardenia Fructus* oil (raw GFO), stir-baked *Gardenia Fructus* oil (stir-baked GFO), and PGFO were provided by Zhejiang Jiaozhi Technology Co., Ltd. Briefly, the ripe fruit of *Gardenia jasminoides* Ellis was harvested in Zhejiang province of China. The fruits were dried in the sun after being inactivated by steaming (120 ℃ for 20–30 min) to obtain the raw GF. Stir-baked GF and praeparatus GF were obtained by roasting the raw GF in a roasting machine with a stainless-steel drum (MSDC-5, Changzhou Jintanmaisi Machinery Co. Ltd, Jiangsu, China), while stir-baked GF (2 kg) was heated at 150 ℃ for 25 min and praeparatus GF (2 kg) was roasted at 200 ℃ for 25 min. After roasting, all the samples were collected and cooled to room temperature. A cold pressing screw expeller (KOMET K300, Hamburg, Germany) was used to press oil from raw GF, stir-baked GF and praeparatus GF, separately. The crude oils were then centrifuged at 8000 rpm for 10 min. The suspended oils were collected as raw GFO, stir-baked GFO, and PGFO, separately and stored at 4 ℃ for further analyses.

2.2 Preparation of fractions of PGFO

PGFO was extracted with *n*-hexane and 90% (*v*/*v*) aqueous methanol (volume ratio 1:1) three times. The *n*-hexane phase was collected and combined, then the *n*-hexane was removed by rotary evaporation at 30–35 ℃ to obtain the lipid fraction of GFO-lipid.

Gardenia Fructus iridoids extract (GFI) and *Gardenia Fructus* crocins extract (GFC) were provided by Zhejiang Suichang Limin Pharmaceutical Co., Ltd (Lishui, Zhejiang, China). Briefly, the *Gardenia Fructus* was extracted with 60% (*v*/*v*) aqueous ethanol and then isolated by HPD 100A column chromatography. GFI was eluted by 20% (*v*/*v*) aqueous ethanol, while GFC was obtained by 80% (*v*/*v*) aqueous ethanol elution, followed by ethanol removal using rotary evaporation at 30–35 ℃. The bioactive components in different fractions of PGFO are shown in Table S1**.**

2.3 Determination of Total Iridoids, Total Crocins, Total Flavonoids, Total Phenolic, and Genipin, Geniposide, Crocetin, and Crocin-1 Content

The total contents of iridoids (TI), crocins (TC), flavonoids (TF), and phenolics (TP) in samples were determined using our previous spectrophotometric methods[24-26]. TI, TC, and TF content were determined by geniposide, crocin-1, rutin, and gallic acid standards, respectively.

The amounts of genipin, geniposide, crocetin, and crocin-1 were analyzed on an Essentia LC-16 liquid chromatography system (Shimadzu, Kyoto, Japan), equipped with a reversed-phase C18 column (Phenomenex Kinetex 5 μm XB-C18 4.6×250mm), as described previously[27]. Genipin and geniposide were

quantified on an Essentia LC-16 (Shimadzu) fitted with a Phenomenex Kinetex XB-C18 column (5 μm, 4.6×250 mm). The mobile phase was 0.1% phosphate buffer (A) and acetonitrile (B) with the following gradient: 0.0–5.0 min, 10%–50% B; 5.0–8.0 min, 50%–95% B, 8.0–12.0 min, 95% B; 12.0–13.0 min, 95%–10% B; 13.0–20.0 min, 10% B. The detection wavelength was 238 nm. Crocetin and crocin-1 were analyzed on the same system using an acetic acid–ammonium acetate buffer (A) and acetonitrile (B) gradient: 0.0–1.0 min, 20% B; 1.10–8.0 min, 20%–60% B; 8.0–8.10 min, 60%–70% B; 8.10–13.0 min, 70%–98% B; 13.10–15.0 min, 98%–20% B; 15.10–20.0 min, 20% B, while detection wavelength was 440 nm.

2.4 Radical Scavenging by DPPH Assay

DPPH scavenging was measured by mixing 2 mL sample with 2 mL 0.101 mM DPPH in ethanol (A_1),[28] with ethanol-only (A_2) and sample-only (A_0) controls. After 1 h at room temperature in the dark, absorbance at 517 nm was recorded. Scavenging activity (%) was calculated as:

$$\text{DPPH} \cdot \text{scavenging activity} = \left(1 - \frac{(A_1 - A_2)}{A_0}\right) \times 100\%$$

2.5 Cell Culture, MTT Assays, and Oxidative Stress Assays

PC12 cells were grown in DMEM + 10% FBS and antibiotics at 37 °C/5% CO_2, with medium changes every other day. Cells were seeded at 1×10^5 cells/mL (100 μL/well in 96-well plates) and allowed to adhere for 24 h. At ~80% confluence, injury was induced by treating cells with 250 μM H_2O_2 for 2 h (Fig. S1A).

PC12 cells were pretreated for 24 h with six concentrations of each test sample—oils (100–600 μg/mL), GFI (10–100 μg/mL), GFC (5–20 μg/mL), crocetin (1–15 μg/mL) and geniposide (1–100 μg/mL). These concentration ranges were selected based on previous study[29] and also based on preliminary cytotoxicity screening using the MTT assay (Fig. S1B–K), which defined the maximum non-cytotoxic dose for each substance in PC12 cells. Parallel assays used concentrations of GFO fractions (GFO-lipid, GFI, GFC, crocetin and geniposide) equivalent to their proportions in the original oil (Table S2). After pretreatment, cells were exposed to 250 μM H_2O_2 for 2 h; untreated cells served as the blank control and H_2O_2-only cells as the injury control.

Cell viability was assessed by MTT assay[30]. After treatment, the medium was replaced with 100 μL of 1 mg/mL MTT in DMEM and incubated for 4 h at 37 °C/5% CO_2. Formazan crystals were dissolved in 150 μL DMSO, and absorbance was measured at 490 nm. Viability was expressed relative to untreated controls. SOD, GSH-Px, CAT activities, MDA, and ROS levels were measured using commercial kits (Beyotime), following the manufacturer's instructions.

2.6 Transcriptomic Analysis and RT-qPCR Validation

Total RNA was extracted from PC12 cells using TRIzol reagent. RNA quality and concentration were assessed using a NanoDrop spectrophotometer and an Agilent 2100 Bioanalyzer. Sequencing libraries were prepared from high-quality RNA samples using the Illumina TruSeq RNA Sample Preparation Kit, which included mRNA enrichment, fragmentation (200–300 bp), and cDNA synthesis with SuperScript II. The libraries were sequenced on an Illumina NextSeq 500 platform.

Raw sequencing reads were quality-filtered using FastQC, and high-quality reads (Q > 30) were aligned to the reference genome using HISAT2 (v2.0.5). Gene counts were obtained using HTSeq (v0.9.1). Differential gene expression analysis was performed using DESeq2 (version 1.30.0). Genes with an absolute $\log_2$ fold change $|\log_2(FC)| > 1$ and an adjusted *P*-value (P) < 0.05 were considered differentially expressed genes (DEGs). Principal component analysis (PCA) was conducted based on the significantly expressed genes. Gene Ontology (GO) enrichment analysis and Kyoto Encyclopedia of Genes and Genomes (KEGG) pathway enrichment analysis of DEGs were performed using the topGO (v2.50.0) and ClusterProfiler (3.4.4) software packages, respectively.

To validate the RNA-seq results, key DEGs were selected for RT-qPCR analysis. Total RNA was reverse-transcribed into cDNA using the PrimeScript RT Reagent Kit. Quantitative real-time PCR (qRT-PCR) was performed on a QuantStudio 7 Real-Time PCR System using SYBR Premix Ex Taq II. The amplification conditions were as follows: 40 cycles of 95 °C for 5 s, 95 °C for 15 s, and 60 °C for 30 s. ACTIN was used as the reference gene for normalization, and the relative gene expression levels were calculated using the $2^{-\triangle\triangle ct}$ method. The primer sequences used are listed in Table S3.

2.7 Animal Study Design and Behavioral Testing

Four-month-old male APP/PS1 transgenic mice and age-matched male wild-type C57BL/6 littermates were obtained from Hangzhou Ziyuan Laboratory Animal Technology Co., Ltd. This research plan has been approved by the Ethics Review Committee of Zhejiang Academy of Agricultural Sciences (2022ZAASLA86), and the experiments were conducted strictly in accordance with the relevant provisions of the Guidelines for the Use and Care of Experimental Animals of Zhejiang Academy of Agricultural Sciences. All animals were housed in a standard barrier facility at the Zhejiang Academy of Agricultural Sciences under controlled conditions (25 ± 2 °C, 50 ± 5% humidity, 12 h light/dark cycle) with free access to standard chow and purified water. After one week of acclimation, mice were randomly divided into four groups (n=6 per group): Control (wild-type, gavaged with purified water), AD (APP/PS1, gavaged with purified water), Positive (APP/PS1, gavaged with donepezil hydrochloride at 0.005 g/kg BW/day), and PGFO (APP/PS1, gavaged with PGFO at 0.5 g/kg BW/day). Interventions were freshly prepared daily and continued for two months during the behavioral testing period. The Morris water maze was used to assess spatial learning and memory. Mice were trained for five days to locate a hidden platform submerged 1–2 cm below opaque white water (24 ± 1 °C), with entry points randomized across quadrants. Mice failing to find the platform within 60 seconds were guided to it. On day six, the platform was removed, and mice explored the pool freely for 60 seconds. A video tracking system recorded escape latency, swim path, platform crossings, and time spent in the target quadrant. The Y-maze, with three equal-length arms at 120° angles, was used to assess spatial working memory. After 30 minutes of acclimation, mice were placed in the maze center and allowed to explore freely for 8 minutes. Arm entries were recorded using a video tracking system. Spontaneous alternation was defined as successive entries into all three arms, and the alternation rate was calculated as:

Alternation rate (%) = (Correct alternations / [Total entries − 2]) × 100%

2.8 Histological Analysis and Biochemical Assessment of Neuroinflammation and Oxidative Stress

Whole brains were fixed in 4% paraformaldehyde at 4 °C for 24 h, followed by graded ethanol dehydration, xylene clearing, and paraffin infiltration. Samples were embedded in paraffin to form tissue blocks and sectioned at 4–6 μm thickness. Sections were mounted and baked at 60 °C for 2 h prior to staining. Sections were dewaxed and rehydrated through xylene (3 × 8 min), graded ethanol (100%, 85%, 75%) and rinsed in tap water. Hematoxylin staining was performed for 6 min, followed by 1 s differentiation in acid alcohol, rinsing, and 15–30 s bluing in ammonia water. Eosin staining was then performed for 10–30 s after brief dehydration in 85% ethanol. Final dehydration was done using graded ethanol and xylene, and sections were sealed with neutral resin for microscopic observation. After dewaxing and rehydration, sections were stained in Nissl solution for 5 min, rinsed three times with distilled water, dehydrated with absolute ethanol, cleared with xylene, and mounted with neutral resin. Neuronal morphology was observed under a microscope and analyzed by image capture.

Cortical tissues were homogenized (10% w/v) in saline and centrifuged at 3500 rpm for 10 min. Supernatants were used to measure MDA, SOD, GSH-PX, and NO levels using commercial kits. Hippocampal tissues were lysed, homogenized, and centrifuged at 13,000 rpm for 10 min. IL-1β, IL-6, and TNF-α levels were determined by ELISA following kit instructions.

2.9 Microbial Composition and Genomic SCFA Analysis

DNA was extracted from the cecal contents of mice using standard protocols. The V3–V4 region of the bacterial 16S rRNA gene was amplified using barcoded primers and TransStart FastPfu DNA Polymerase. PCR products were pooled, purified, and quantified. Equimolar amplicons were used to construct sequencing libraries. Libraries were prepared and sequenced on the Illumina platform (Illumina, USA), yielding an average of 50,000 high-quality reads per sample after quality control. For bioinformatic analysis, the sequencing reads were processed by quality filtering, denoising to generate amplicon sequence variants (ASVs), and removal of chimeric sequences. Taxonomic assignment of ASVs was performed using the SILVA database (v138). Prior to diversity analysis, the ASV table was rarefied to an even depth across samples. Alpha diversity indices (Ace, Chao, Shannon) and beta diversity (assessed by Principal Coordinates Analysis based on Bray-Curtis distances) were subsequently calculated. Cecal contents were homogenized in sterile water with isocaproic acid as an internal standard, then centrifuged and extracted with sulfuric acid and diethyl ether. After filtration and a second centrifugation, supernatants were analyzed by gas chromatography. Column temperature was programmed from 100 °C to 150 °C at 2 °C/min. SCFA concentrations were determined using standard curves.

2.10 Statistical Analysis

Results were reported as the mean ± standard deviation (SD). The independent sample size n in the experiment is defined as follows: n represents the number of independent biological replicates based on different cell culture batches *in vitro* cell experiments; The n *in vivo* animal experiments represents the number of independent mice in each experimental group; The n in microbiome analysis represents the number of

independent mouse fecal samples. SPSS version 25.0 software was used for all statistical calculations. ANOVA was used to determine the differences between the sample results. All values with $P < 0.05$ were considered statistically significant.

3. Results

3.1 Phytochemical Composition and In Vitro Neuroprotective Activity of Raw, Stir-Baked, and Praeparatus Gardenia Fructus Oils

Raw GFO, stir-baked GFO, and PGFO were prepared as presented in Fig. 1A. The different roasted GF, their oil products as well as other experiment oil are shown in Fig. 1B–C. As shown in Table 1, three GFOs contain unique components, i.e., TI (25.16–41.22 μg/mg) and TC (0.43–2.09 μg/mg) only exist in GFOs, not in the other three common edible oils. Among three different GFOs, PGFO showed a significantly higher level of TI and TC than that in raw GFO and stir-baked GFO. As for the individual compounds shown in Fig. S2 and Table 1, geniposide and genipin (the aglycone of geniposide) were the main iridoids in GFOs; Crocein was the only crocins detected in three GFOs. Similarly, the content of all three bioactive compounds was enhanced with the increase of roasting temperature on GF. When compared to raw GFO, PGFO contained 1.2-, 2.1-, and 2.5-fold higher content of genipin, geniposide, and crocetin, respectively.

Table 1. Content of Bioactive components in different roasted GFOs and three edible oils

Compounds	Raw GFO	Stir-baked GFO	Praeparatus GFO	Rapeseed oil	Olive oil	Soybean oil
Total iridoids (μg/mg)	25.16 ±0.53^{b}	25.25 ±1.22^{b}	41.22 ±2.21^{a}	ND	ND	ND
Total crocins (μg/mg)	0.45 ±0.03^{b}	0.43 ±0.03^{b}	2.09 ±0.13^{a}	ND	ND	ND
Total flavonoids (μg/mg)	1.04 ±0.03^{c}	1.00 ±0.09^{c}	1.89 ±0.09^{a}	0.61 ±0.02^{d}	1.56 ±0.01^{b}	0.98 ±0.11^{c}
Total phenols (μg/mg)	1.51 ±0.04^{d}	1.90 ±0.10^{c}	5.40 ±0.04^{a}	ND	3.96 ±0.07^{b}	ND
Genipin (μg/g)	26.07 ±0.07^{b}	26.07 ±0.11^{b}	30.58 ±0.79^{a}	ND	ND	ND
Geniposide (μg/g)	80.18 ±2.34^{b}	88.36 ±1.43^{b}	168.42 ±6.46^{a}	ND	ND	ND
Crocetin (μg/g)	10.52 ±0.16^{c}	13.45 ±0.79^{b}	26.30 ±0.02^{a}	ND	ND	ND

Indicator: Lowercase letters (series "$^{a-d}$") indicate significant differences ($P < 0.05$) between different samples. ND means not detected.

In vitro antioxidant activity of oil samples was determined by DPPH radical assays. The DPPH radical scavenging effect of different concentrations of GFO and three edible oils was shown in Fig. 1D. As the concentration of oil samples increased, the scavenging rate of DPPH increased gradually, and PGFO showed the highest *in vitro* antioxidant capacity in six oil samples (IC_{50} 2.34 mg/mL), compared to other oil types.

Viability of H_2O_2-injured PC12 cells was used for investigating the protective effects of raw GFO, stir-baked GFO, PGFO, rapeseed oil, olive oil, and soybean oil. As shown in Fig. 1E, the cells pretreated with olive oil, soybean oil, and GFO samples showed reduced H_2O_2-induced cell toxicity in a dose-dependent manner. Furthermore, GFOs, especially PGFO, showed a significantly better protective effect on PC12 cells

than other edible oils. At the concentration of 600 μg/mL, PGFO could restore the cell viability up to 86.92% (a 30.67% enhancement compared to the H_2O_2 injury group), followed by stir-baked GFO (18.38%) and raw GFO (17.38%).

Based on these findings, PGFO demonstrated the most potent neuroprotective and antioxidant efficacy among all tested oil samples. Therefore, it was selected as the primary candidate for all subsequent investigations to elucidate its underlying mechanisms of action.

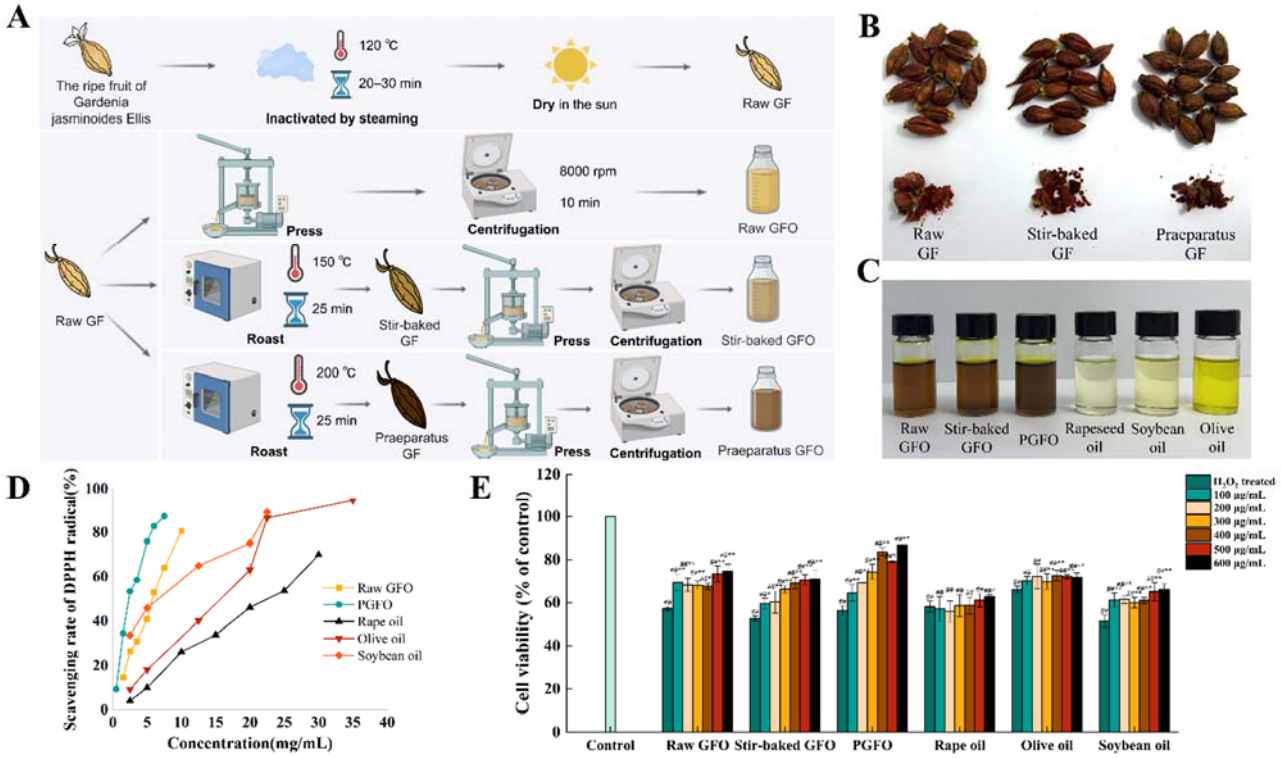

Fig. 1. (**A**) Preparation process diagram of raw GFO, stir-baked GFO and PGFO. (**B**) GF with different roasting temperatures. (**C**) Six oil samples. (**D**) Radical scavenging activity of GFOs and three edible oils in different concentrations, given as percentage inhibition (n=6). (**E**) Effects of raw GFO, stir-baked GFO, PGFO, rapeseed oil, olive oil, and soybean oil on the cell viability of PC12 cells in H_2O_2 induced toxicity (n=6). The data are represented as mean ± SD. ## means $P < 0.01$ compare to control. * means $P < 0.05$, ** means $P < 0.01$ compare to H_2O_2 injury group.

3.2 Evaluation of PGFO Fractions and Major Constituents for Cytoprotection in H_2O_2-Injured PC12 Cells and Antioxidant Activity of PGFO

To further clarify which components in PGFO exert cytoprotective effects on PC12 cells, three fractions (GFO-lipid, GFI, and GFC) and two main detected bioactive compounds (crocetin and geniposide) were selected and investigated for their protective effects on PC12 cells damaged by H_2O_2, respectively. Brief preparation of GFO-lipid, GFI, and GFC was shown in Fig. 2A. Based on the high purity levels of both GFI and GFC (above 80%) (Table S1), the equivalent concentrations for each fraction and compound applied to PC12 cells were also calculated and applied (Table S2) according to their amounts in PGFO (Table 1).

Table 1. Content of Bioactive components in different roasted GFOs and three edible oils

Compounds	Raw GFO	Stir-baked GFO	PraeparatusGFO	Rapeseedoil	Olive oil	Soybean oil
Total iridoids (μg/mg)	25.16±0.53^b	25.25±1.22^b	41.22±2.21^a	ND	ND	ND
Total crocins (μg/mg)	0.45±0.03^b	0.43±0.03^b	2.09±0.13^a	ND	ND	ND

Total flavonoids (μg/mg)	1.04±0.03^{c}	1.00±0.09^{c}	1.89±0.09^{a}	0.61±0.02^{d}	1.56±0.01^{b}	0.98±0.11^{c}
Total phenols (μg/mg)	1.51±0.04^{d}	1.90±0.10^{c}	5.40±0.04^{a}	ND	3.96±0.07^{b}	ND
Genipin (μg/g)	26.07±0.07^{b}	26.07±0.11^{b}	30.58±0.79^{a}	ND	ND	ND
Geniposide (μg/g)	80.18±2.34^{b}	88.36±1.43^{b}	168.42±6.46^{a}	ND	ND	ND
Crocetin (μg/g)	10.52±0.16^{c}	13.45±0.79^{b}	26.30±0.02^{a}	ND	ND	ND

Indicator: Lowercase letters (series "$^{a–d}$") indicate significant differences ($P < 0.05$) between different samples. ND means not detected.

However, in all these bioactive fractions or compounds, almost no cytoprotective effect was observed (Fig. 2B–F). Only GFI, at the concentration of 30 μg/mL (equivalent amount of 600 μg/mL PGFO), improved the cell survival rate by 9.88 % compared to the H_2O_2-treated group, much lower than that of PGFO (30.67%) shown above (Fig. 1E and Fig. 2B). However, our data demonstrated that GFI (5–100 μg/mL), GFC (3–20 μg/mL), geniposide (1–100 μg/mL), and crocetin (1–15 μg/mL) showed similar protective effects at much higher and safe concentrations (Fig. S3 A–D), indicating lipid fraction in PGFO could improve the bioactivity of these fraction and bioactive compounds.

Pretreatment with PGFO markedly reduced the relative ROS and MDA levels in PC12 cells (Fig. 2G–H). The human body has a natural defense system against oxidative damage, with antioxidant enzymes such as GSH-Px, SOD, and CAT playing a critical role. Pretreatment with PGFO brought an obvious increase in antioxidant enzymes in PC12 cells (Fig. 2I–K).

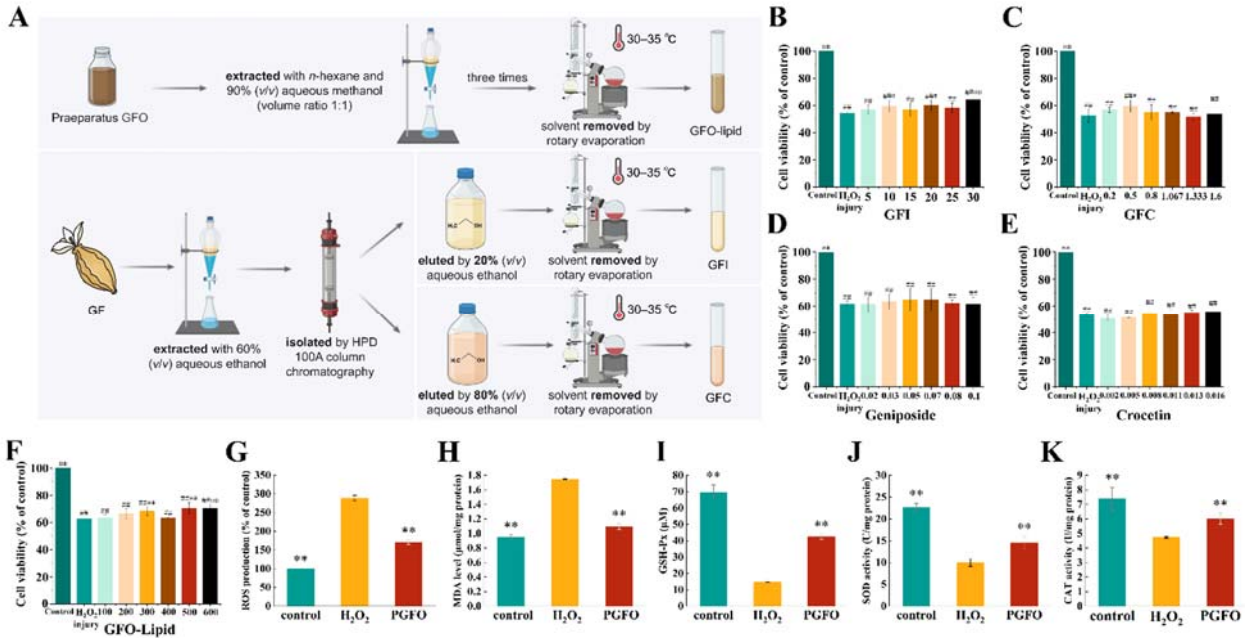

Fig. 2. (**A**) Preparation of PGFO different fractions. The effects of equivalent concentrations of (**B**) GFI, (**C**) GFC, (**D**) GFO-lipid, (**E**) crocetin, and (**F**) geniposide on the survival rate of PC12 cells induced by H_2O_2 (n=6). Effects of PGFO on the oxidative stress of PC12 cells (**G**) ROS levels, (**H**) MDA levels, (**I**) GSH-Px activity, (**J**) SOD activity, and (**K**) CAT activity (n=6). The data are represented as mean ± SD. ## means $P < 0.01$ compare to control. * means $P < 0.05$, ** means $P < 0.01$ compare to H_2O_2 injury group.

3.3 Transcriptomic Profiling Identifies Key Signaling Pathways Underlying PGFO–Mediated Neuroprotection

The PCA analysis of RNA-seq results demonstrated that three groups can be distinguished clearly (Fig. S4). Gene expression levels of control, H_2O_2 injury, and PGFO groups were quantified and compared. The heatmap of the top 30 DEGs is shown in Fig. 3A.

To identify the specific biological pathways involved in the protective effect of PGFO against H_2O_2-injured PC12 cells, a comprehensive KEGG enrichment analysis was performed for each comparison group by using DEGs. From this analysis, several key signaling pathways of H_2O_2-injured cells emerged, such as cell cycle (rno04110), DNA replication (rno03030), ECM-receptor interaction (rno04512), and PI3K-Akt signaling pathway (rno04151). (Fig. 3B) Among them, the PI3K-Akt signaling pathway showed the highest DEGs enrichment and was reported to have a strong correlation with neurodegenerative diseases caused by oxidative stress[31]. In the comparison between the PGFO group and the H_2O_2 injury group, the top 20 significantly enriched canonical pathways of DEGs were identified (Fig. 3C). Among them, the neuroactive ligand–receptor interaction and tryptophan metabolism pathways were particularly notable, as both are closely associated with neurodegenerative diseases[32, 33].

Consistently, five DEGs—PLG, AGT, COL11A1, TPH2, and CYP1A1—which ranked among the top 30 DEGs (Fig. 3A), were mapped to these two pathways. To further validate their involvement, these DEGs were selected for RT-qPCR analysis, and the results confirmed their differential expression (Fig. 3D–H).

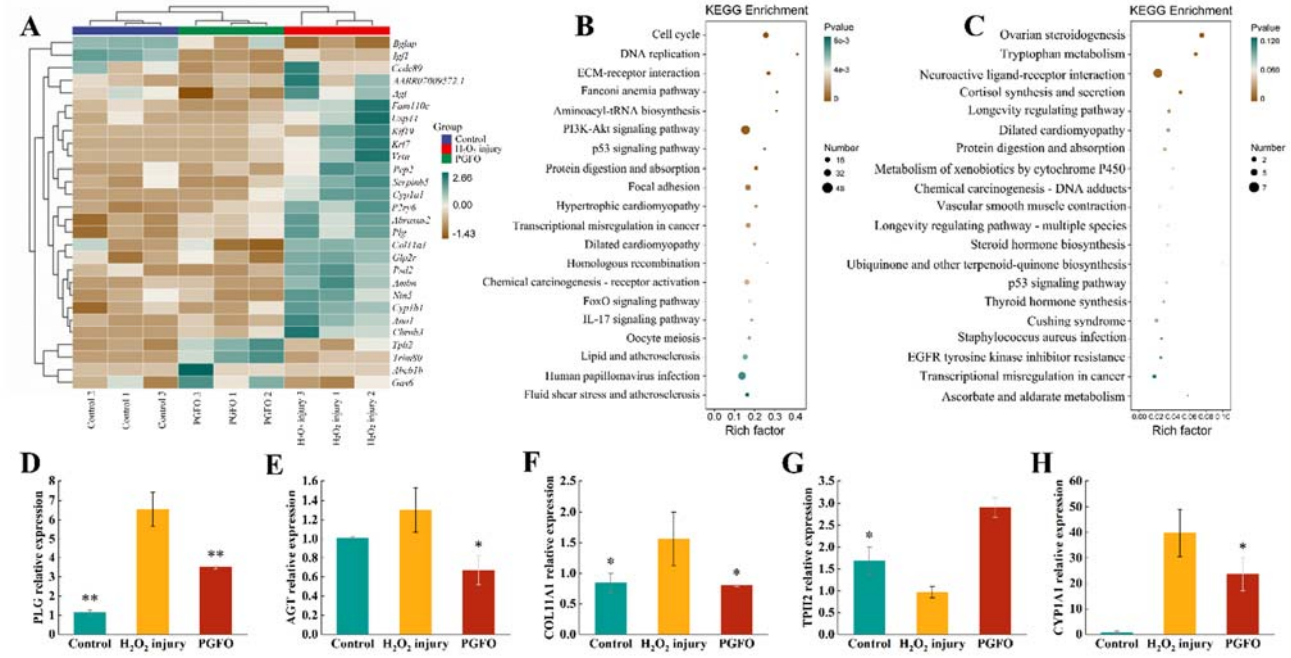

Fig. 3. (**A**) The heatmap representation of the top 30 DEGs changed mRNA transcripts in PC12 cells (n=6). (**B** and **C**) The top 20 canonical pathways by KEGG enrichment analysis of DEGs (n=6). The size of the dot in the figure indicated the number of DEGs was annotated to the pathway and the color represented P value of the pathway. RT-qPCR analysis was performed to validate RNA-seq data, with five DEGs selected: (**D**) PLG, (**E**) AGT, (**F**) COL11A1, (**G**) TPH2, and (**H**) CYP1A1 (n=3). The data are represented as mean ± SD. * means $P < 0.05$, ** means $P < 0.01$ compare to H_2O_2 injury group.

3.4 PGFO Ameliorates Cognitive Impairment and Neurodegeneration in APP/PS1 Mice via Antioxidant and Anti-Inflammatory Mechanisms

Since PGFO exhibited protective effects on PC12 cells, we further employed APP/PS1 transgenic mice to investigate its activity *in vivo* and to determine whether PGFO confers protective effects in a brain disease

model. Progressive cognitive decline is a hallmark of AD. To assess cognitive function, the Morris water maze was used. During training, escape latency gradually decreased in both the Positive and PGFO groups (Fig. 4A). By day 5, PGFO-treated mice reached the platform in 23.51 s—significantly faster than AD mice (50.62 s), while Control mice took 15.78 s. Trajectory analysis further showed that PGFO mice exhibited markedly improved spatial navigation compared to the AD group (Fig. 4B). After platform removal, both the Positive and PGFO groups showed significantly more platform crossings (Fig. 4C), spent more time in the target quadrant (Fig. 4D), and reached the former platform location faster (Fig. 4E) compared to the AD group. Representative trajectory maps during the test (Fig. 4F) showed that Control, Positive, and PGFO group mice exhibited continuous exploration of the platform's location, while AD group mice displayed aimless movement patterns.

The Y-maze test evaluates spatial working memory by measuring spontaneous alternations. Successive entries into all three arms reflect good memory performance. Movement trajectories (Fig. 4G) and spontaneous alternation rates (Fig. 4H) showed PGFO effectively enhanced memory function impaired by AD (PGFO: 47.42±7.57% vs. AD: 31.38±7.00%).

Hematoxylin–eosin (HE) staining provides clear morphological visualization of neuronal structures, enabling the assessment of tissue organization and pathological alterations. As shown in Fig. 4I, the Control group displayed intact cortical architecture with orderly neuronal arrangements and no evident abnormalities. In contrast, the AD group exhibited reduced neuronal density, nuclear hyperchromasia, and disorganized structures, indicating neurodegeneration. Treatment with PGFO improved neuronal morphology and restored tissue organization toward normal. Nissl staining highlights neuronal integrity by visualizing Nissl bodies, which reflect protein synthesis activity. A reduced number or loss of Nissl bodies indicates neuronal damage. In Fig. 4J, Control group neurons showed abundant, dark-stained Nissl bodies with clear morphology. In contrast, the AD group exhibited reduced and faintly stained Nissl bodies, especially in the cortex and hippocampal CA3 region. Both Positive and PGFO treatments increased Nissl body number and staining intensity, indicating partial neuronal protection or restoration. To evaluate PGFO’s effect on the antioxidant system, cortical SOD, MDA, and GSH-PX levels were measured. AD mice showed impaired antioxidant capacity, with reduced SOD and GSH-PX activities and elevated MDA levels. PGFO treatment significantly improved these markers, indicating enhanced oxidative stress resistance (Fig. 4K–M). TNF-α, IL-6, and IL-1β are key proinflammatory cytokines involved in neuroinflammation. ELISA results showed that while donepezil significantly reduced hippocampal TNF-α levels, PGFO exhibited a mild, non-significant reduction. Both treatments markedly decreased elevated IL-6 and IL-1β levels in AD mice, indicating anti-inflammatory effects (Fig. 4N–P).

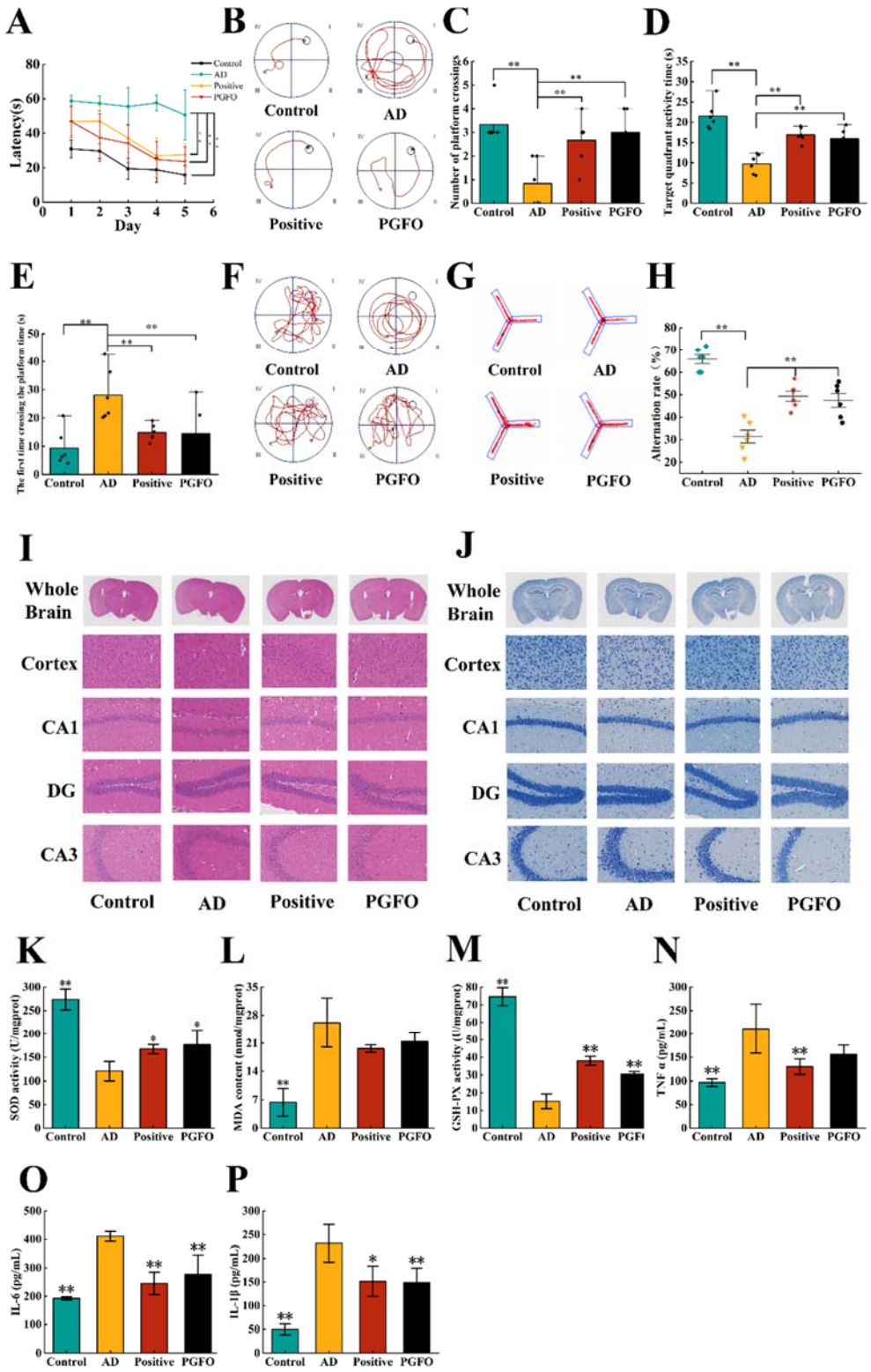

Fig. 4. (**A**) Successful escape incubation period lasting for five days of training (n=6). (**B**) Representative diagram of mouse swimming trajectory on the fifth day of training (n=6). (**C**) Number of platform crossings during the detection phase (n=6). (**D**) Target quadrant activity time during the detection phase (n=6). (**E**) The time of the first crossing of the platform during the detection phase (n=6). (**F**) Representative diagram of mouse swimming trajectory during the detection phase (n=6). (**G**) Representative motion trajectory maps of mice in each group in the Y-maze (n=6). (**H**) Alternating success rate in Y-maze experiment of mice in each group (n=6). (**I**) Effect of PGFO on HE staining results in brain tissue of APP/PS1 mice. (**J**) Effect of PGFO on Nissl staining results in brain tissue of APP/PS1 mice. Whole Brain: the entire brain area of mice; Cortex: cortical region of mouse brain tissue; CA1: The CA1 region of the mouse hippocampus; DG: DG region of mouse hippocampus; CA3: The CA3 region of the mouse hippocampus (2500 μm and 100 μm). The effect of PGFO on the levels of oxidative stress (**K**) SOD activity, (**L**) MDA content, and (**M**) GSH-PX activity in the cortex of APP/PS1 mice (n=3). The effect of gardenia fruit oil on the content of three pro-inflammatory factors (**N**) TNF-α, (**O**) IL-6, and (**P**) IL-1β in APP/PS1 mice (n=3). The data are represented as mean ± SD. * represents a significant difference compared to the AD group (* $P < 0.05$, ** $P < 0.01$).

3.5 Regulatory Effect of PGFO on Intestinal Flora in APP/PS1 Mice

Based on the hypothesis that plant derived components may exert cross-border regulatory effects through gut microbiota, this study further explores the effects of PGFO on gut microbiota and metabolites in APP/PS1 mice to verify its potential mediating pathway for neuroprotective effects.

Alpha diversity of the intestinal microbiota was evaluated using Ace, Chao, and Shannon indices. Both richness (Ace, Chao) and diversity (Shannon) were significantly reduced in AD mice and improved following treatment with donepezil or PGFO (Fig. 5A–C).

To assess overall microbial community structure, PCoA was performed. The AD group showed distinct separation from the Control group, indicating substantial alterations in microbial composition (Fig. 5D). Notably, the PGFO and Positive groups were shifted away from the model group and closer to the Control group, suggesting that PGFO attenuated AD-associated gut microbiota dysbiosis. At the phylum level, Bacillota was elevated in AD mice, while Actinomycota was enriched in the PGFO group. Thermodesulfobacteriota levels, reduced in AD mice, were restored by donepezil and PGFO. Other phyla showed no significant differences among groups (Fig. 5E–G).

To further assess the impact of PGFO on gut microbiota, genus-level analysis was conducted. The dominant genera included *norank_f_Muribaculaceae*, *Allobaculum*, *Lactobacillus*, *unclassified_f_Lachnospiraceae*, and *Ileibacterium* (Fig. S5). Muribaculaceae abundance was lower in all AD-related groups, though slightly increased with PGFO (Fig. 5H). *Allobaculum* and *Lactobacillus* were elevated in the AD group but markedly reduced by PGFO and donepezil (Fig. 5I–J). Lachnospiraceae levels were higher in Control, Positive, and PGFO groups but showed no significant difference (Fig. 5K). *Ileibacterium* was abundant only in the Control group (Fig. 5L). SCFA levels in cecal contents were measured to assess microbial metabolic function. AD mice showed significantly reduced levels of propionic acid, acetic acid, isovaleric acid, n-butyric acid, and n-valeric acid compared to Controls. PGFO treatment significantly increased all SCFAs except acetic acid, which showed an upward trend without statistical significance (Fig. 5M–Q). In this study, PGFO significantly increased the levels of SCFAs in the cecum of APP/PS1 mice and was positively correlated with the abundance of acid producing bacteria such as Lachnospiraceae, suggesting that gut microbiota metabolites may be a key mediator for PGFO to exert cross-border regulatory effects. To explore the link between gut microbiota and their metabolites, a correlation analysis was conducted between SCFA levels and bacterial genera (Fig. S6). Among them, the relative abundances of genera such as *unclassified_f__Lachnospiraceae*, *unclassified_f__Ruminococcaceae*, *Lachnospiraceae_NK4A136_group*, *norank_o__Clostridia_UCG-014*, *norank_f__Desulfovibrionaceae*, *Muribaculum*, *unclassified_f__Oscillospiraceae*, *Alistipes*, *Odoribacter*, and *Butyribacter* were positively correlated with the content of SCFAs, indicating that such genera may directly participate in the production of SCFAs through their metabolic activities. The relative abundances of genera such as *Lactobacillus*, *Bifidobacterium*, *Dubosiella*, *unclassified_c__Bacilli*, and *Faecalibaculum* were negatively correlated with the content of SCFAs.

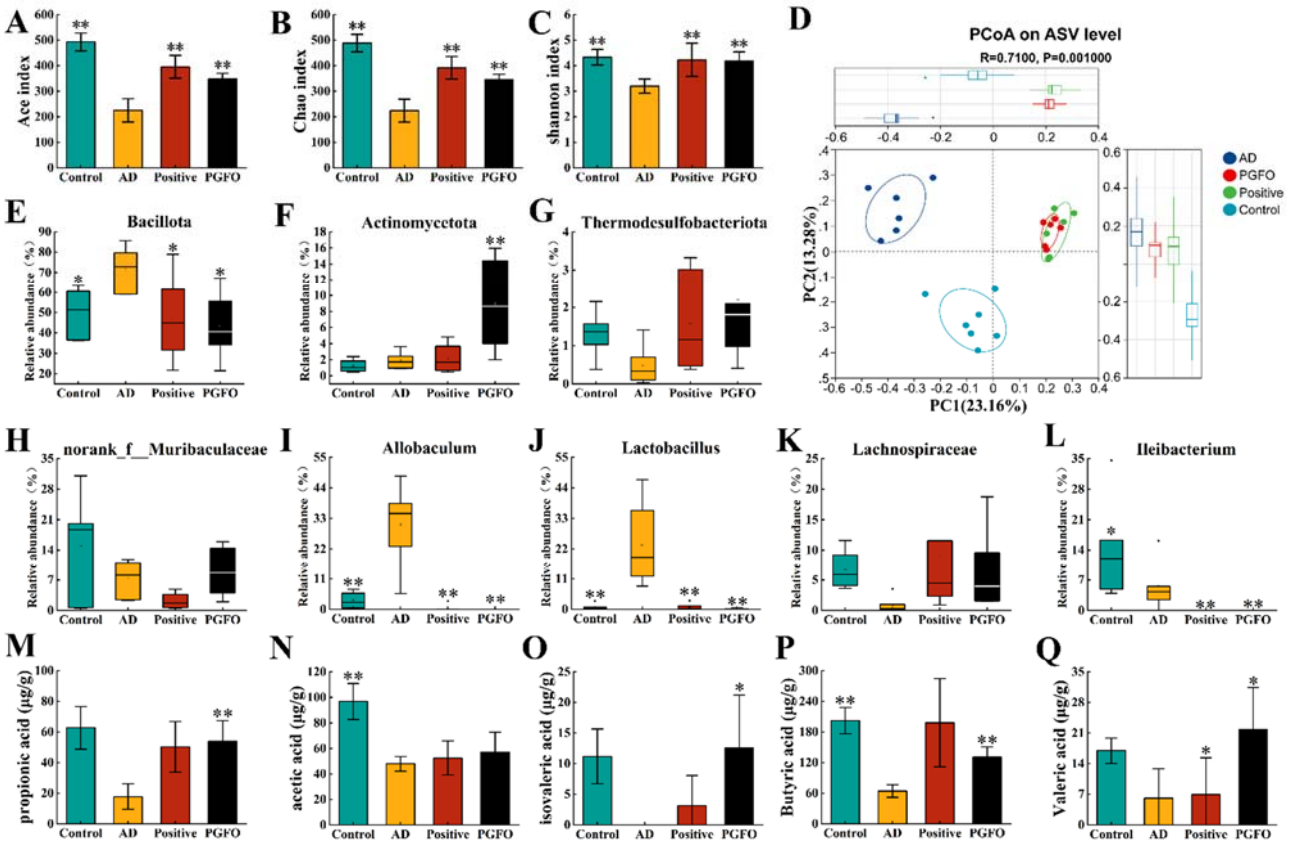

Fig. 5. The effect of PGFO on alpha diversity indices. (**A**) Ace index, (**B**) Chao index, (**C**) Shannon index (*n*=6). (**D**) Effect of PGFO on beta diversity of gut flora in APP/PS1 mice (*n*=6). (**E**–**G**) Relative abundance of mouse gut microbiota at the phylum level (*n*=6). (**H**–**L**) Relative abundance of the top five genera in mouse gut microbiota ranking (*n*=6). The effect of PGFO on five SCFAs of (**M**) Propionic acid, (**N**) Acetic acid, (**O**) Isovaleric acid, (**P**) Butyric acid, (**Q**) Valeric acid in cecal contents of APP/PS1 mice (*n*=6). The data are represented as mean ± SD. * represents a significant difference compared to the AD group (* $P < 0.05$, ** $P < 0.01$).

4. Discussion

As life expectancy increases, the prevalence of neurodegenerative diseases is also rising[34], with oxidative stress and inflammation recognized as key contributors to neuronal cell death[35]. Dietary interventions, particularly functional edible oils, play an important role in slowing disease progression[36]. In this context, the present study demonstrates that PGFO possesses superior neuroprotective properties compared to raw or stir-baked GFO, as well as common edible oils such as rapeseed, olive, and soybean oil. This enhanced efficacy is attributable, at least in part, to its higher content of bioactive constituents, such as crocetin and geniposide, which are generated or concentrated during the roasting process[37-39]. Among the three GFOs examined, PGFO contained the highest levels of these compounds and correspondingly exhibited the most potent cytoprotective activity in H_2O_2-injured PC12 cells, underscoring the importance of processing parameters in optimizing the bioactivity of *Gardenia Fructus*-derived products. This finding is consistent with the general laws in the field of food processing. For instance, studies have confirmed that roasting can significantly increase the contents of phytosterols, tocopherols, and carotenoids in peanut oil, as well as enhance its antioxidant activity[40]. Similarly, stir-baking Fructus Aurantii with bran can increase the content of its active component auraptene, thereby improving its efficacy in invigorating the spleen and relieving abdominal distension[33].

Unlike conventional polyphenol-rich edible oils that have been investigated for neuroprotective properties, such as olive oil which is characterized by high levels of hydroxytyrosol and oleuropein[41], or sea buckthorn oil which has been shown to improve cognitive function in APP/PS1 mice through antioxidant and anti-inflammatory mechanisms[42], PGFO possesses a distinct phytochemical profile. Its neuroprotective effects are mediated by a unique combination of iridoids (geniposide, genipin) and apocarotenoids (crocetin), compounds rarely found in dietary oils. Moreover, while the neuroprotective effects of oils like olive oil are primarily attributed to phenolic compounds acting through antioxidant pathways, PGFO engages additional mechanisms, including modulation of the tryptophan/serotonin/melatonin axis and regulation of the gut microbiota–SCFAs–brain axis. This multi-faceted mechanism of action distinguishes PGFO from other functional oils and positions it as a particularly promising candidate for dietary intervention in neurodegenerative diseases.

Interestingly, while the main bioactive components of PGFO—GFI, GFC, geniposide, and crocetin significantly improved the survival of H_2O_2-injured PC12 cells within their safe concentration ranges, their protective effects were limited when applied in equivalent amounts as present in PGFO. Similarly, the lipid fraction alone showed minimal cytoprotective activity. In contrast, the complete PGFO matrix exhibited strong protective effects. This difference points to a synergistic interaction among constituents within the oil matrix. Several mechanisms may account for this synergy. The lipid-rich environment of PGFO may function as a natural delivery vehicle, enhancing the solubilization and intestinal absorption of hydrophilic compounds such as geniposide. For instance, the poor bioavailability of ursolic acid could be completely changed by co-processing with edible oil[43], and lipids can improve the bioavailability of carotenoids[44].As dietary lipids are key modulators of diet-microbiota interactions[45], the lipid matrix of PGFO may alter the composition of gut microbiota, thereby promoting the microbial biotransformation of iridoid glycosides into more bioactive metabolites that further enhance neuroprotective potential[46]. These hypotheses provide a framework for future investigations aimed at dissecting the molecular basis of matrix-dependent synergy in functional oils.

To further elucidate the antioxidant mechanism of PGFO in PC12 cells, RNA sequencing was conducted. PGFO pretreatment notably enriched DEGs in the neuroactive ligand–receptor interaction pathway—critical for neurotransmission and neural function[47]. Downregulation of AGT, COL11A1, and PLG in the PGFO group compared to the H_2O_2 group is particularly relevant. AGT and COL11A1 are identified as Alzheimer's disease susceptibility genes, while PLG is a known modulator of neuroinflammation and Aβ peptide degradation[48-50]. In the AD model, reduced expression of PLG is associated with attenuated immune activation and decreased Aβ accumulation[49]. Therefore, the downregulation of these genes observed in our study suggests that the neuroprotective mechanism by which PGFO alleviates oxidative damage and inflammation may partially involve the regulation of these pathways related to neuroinflammation and Aβ pathology. These observations suggest that the neuroprotective mechanism of PGFO may involve regulation of genes linked to neuroinflammation and Aβ pathology.

In parallel, the tryptophan (Trp) metabolism pathway was also significantly enriched in the PGFO-treated group. Trp metabolism plays a critical role in numerous neuropsychiatric disorders through three major pathways: the serotonin (5-HT), kynurenine, and indole pathways[51]. In our study, DEGs enriched in the tryptophan metabolism pathway were primarily associated with the 5-HT pathway. PGFO treatment upregulated *TPH2*, which encodes the rate-limiting enzyme in serotonin biosynthesis, while downregulating *CYP1A1* and *CYP1B1*, cytochrome P450 enzymes involved in melatonin catabolism[52]. This expression pattern points to a potential enhancement of the tryptophan/serotonin/melatonin axis. Serotonin is a key neurotransmitter involved in mood regulation, cognition, and stress response[53], while melatonin regulates circadian rhythms and exerts antioxidant effects[54]. This modulation of the 5-HT pathway likely contributes to the neuroprotective effects of PGFO. Together, these transcriptomic findings, while requiring protein-level validation, provide a molecular framework for understanding the direct central actions of PGFO.

PGFO demonstrated robust neuroprotective effects in the APP/PS1 mouse model of AD. Chronic oxidative stress and neuroinflammation are key pathological features of AD that jointly drive synaptic dysfunction and neuronal loss[55]. In this study, chronic administration of PGFO significantly improved cognitive performance and preserved neuronal integrity, as evidenced by behavioral tests and histological examination. Biochemically, PGFO restored the cortical antioxidant defense system and attenuated hippocampal neuroinflammation. The NLRP3 inflammasome has been recognized as a central mediator of neuroinflammation in AD[56]. Whether PGFO exerts its anti-inflammatory effects through modulation of this pathway warrants further investigation. These findings establish that PGFO confers cognitive and neuroprotective benefits in a clinically relevant AD model.

Another finding is the impact of PGFO on gut microbiota composition in AD mice. Growing evidence links gut microbiome dysbiosis to AD progression *via* the gut–brain axis[57]. In the study, PGFO treatment partially reversed AD-associated gut microbiota dysbiosis, as reflected by increased alpha diversity, shifted community structure toward healthy controls, and altered abundance of key genera including *Allobaculum*, *Lactobacillus*, and SCFA-producing taxa such as *Lachnospiraceae*.

These findings are consistent with previous reports demonstrating that gut microbiota composition is altered in response to neurodegenerative pathology and that such dysbiosis can be partially restored by dietary interventions. For example, the *Allobaculum* level was reported to be significantly elevated in APP/PS1 mice compared to wild-type controls, and walnut peptide supplementation decreased the *Allobaculum* level and improved cognitive function[58]. Similarly, feeding *Lactobacillus* plantarum DACNJS22 to neurologically impaired mice increased the abundance of *Lachnospiraceae*[59], a genus often associated with anti-inflammatory effects. For example, *Lachnospiraceae_NK4A136_group* is generally considered a producer of SCFAs[60], which have also been reported to support brain health and restrain the overgrowth of pro-inflammatory microbes that produce endotoxins[61].

Consistent with these compositional changes, PGFO significantly elevated cecal levels of multiple SCFAs, with positive correlations observed between SCFA-producing genera and SCFA concentrations. The

simultaneous observation of elevated cecal SCFAs and attenuated hippocampal neuroinflammation in PGFO-treated mice raises the possibility of a mechanistic link between these two phenomena. SCFAs, particularly butyrate and propionate, are known to traverse the blood-brain barrier and directly suppress microglial activation[61, 62]. This evidence strongly suggests that the anti-inflammatory effects of PGFO in the brain may be mediated, at least in part, via the gut microbiota–SCFAs–brain axis. This interpretation is further substantiated by the positive correlation observed between SCFA-producing genera and SCFA levels in our study, supporting the notion that PGFO-induced changes in gut microbiota composition could causally contribute to the attenuation of neuroinflammation.

Based on the aforementioned *in vitro* and *in vivo* findings, the neuroprotective effects of PGFO may be synergistically achieved through a dual pathway involving both direct central actions and indirect gut-brain axis modulation. On one hand, geniposide and trans-crocetin (the intestinal metabolite of crocins) have been confirmed to cross the blood-brain barrier[63, 64], potentially entering the central nervous system directly to exert antioxidant and anti-inflammatory effects. On the other hand, through remodeling of the gut microbiota and subsequent elevation of SCFAs, PGFO engages the gut–brain axis to suppress neuroinflammation.

Several limitations of the present study should be acknowledged. First, the transcriptomic findings, while suggestive of pathway engagement, require validation at the protein level to confirm functional relevance. Western blot or immunohistochemical analysis of key nodes within the neuroactive ligand–receptor interaction pathway (e.g., AGT, PLG) and the tryptophan metabolism pathway (e.g., TPH2, CYP1A1) would strengthen the mechanistic conclusions. Second, the proposed relationship between gut microbiota remodeling and neuroinflammation, while supported by correlational data and established SCFA biology, needs definitive proof through functional experiments. Future studies employing faecal microbiota transplantation from PGFO-treated donors into germ-free or antibiotic-treated AD mice, or targeted depletion of specific microbial taxa, would help establish causality. Third, while the synergistic interaction among PGFO constituents is inferred from the difference between intact oil and isolated fractions, the specific combinations responsible for this synergy and their molecular targets remain to be dissected. Addressing these questions through systematic reconstitution experiments and pathway-specific inhibitors will be essential for advancing the development of PGFO-based functional oil products.

In conclusion, this study demonstrates that PGFO exhibits superior neuroprotective activity both *in vitro* and *in vivo*. Its efficacy appears to derive from a combination of factors: a high content of bioactive constituents, synergistic interactions within the oil matrix, and a mechanism involving both direct central modulation and indirect regulation via the gut–brain axis. These findings provide a theoretical foundation for the development of PGFO as a functional dietary ingredient for neurodegenerative diseases.

5. Conclusion

Among the three processed GFOs, PGFO exhibited the highest levels of the active compounds—geniposide, genipin, and crocetin—and showed superior antioxidant capacity. In H_2O_2-injured PC12 cells, PGFO significantly improved cell viability, reduced ROS and MDA levels, and enhanced

antioxidant enzyme activities (SOD, GSH-Px, CAT). Isolated fractions and individual compounds demonstrated limited protection compared to the complete PGFO, suggesting synergistic effects among its constituents. Transcriptomic and RT-qPCR analyses indicated that PGFO may modulates neuroprotective pathways, notably the neuroactive ligand–receptor interaction and tryptophan metabolism pathways, with gene changes indicative of enhanced serotonergic signaling and reduced inflammation. *In vivo*, PGFO improved cognition, preserved neuronal morphology, restored antioxidant balance, reduced neuroinflammation, and partially corrected gut microbiota dysbiosis in APP/PS1 mice. This multi-target profile addresses both central and peripheral contributors to AD, supporting PGFO's potential as a functional dietary oil for neuroprotection and AD prevention. Overall, this study provides mechanistic insights into PGFO's neuroprotective actions and establishes a theoretical foundation for its development as a functional food ingredient in the prevention and management of neurodegenerative diseases.

Declaration of competing interest

The authors confirm that they have no conflicts of interest with respect to the work described in this manuscript.

Date availability

Data will be made available on request.

Acknowledgement

This work was supported by the National Natural Science Foundation of China (No.32502213), General Scientific Research Project of the Zhejiang Provincial Department of Education (Grant No. Y202456700); Ningbo University (Grant No. 422303463); One Health Interdisciplinary Research Project, Institute of One Health, Ningbo University; Zhejiang Provincial Natural Science Foundation of China (grant number ZCLQN26C2001).

References

[1] A. Ruqayya, R.M. Habibur, S. Kyoungho, Implications of glial metabolic dysregulation in the pathophysiology of neurodegenerative diseases, Neurobiology of disease. 174 (2022) 105874. https://doi.org/https://doi.org/10.1016/j.nbd.2022.105874.

[2] S. Kaur, H. Verma, M. Dhiman, A.K. Mantha, Activation of multifunctional DNA repair APE1/Ref-1 enzyme by the dietary phytochemical Ferulic acid protects human neuroblastoma SH-SY5Y cells against Aβ (25–35)-induced oxidative stress and inflammatory responses, Mitochondrion. 79 (2024) 101947. https://doi.org/10.1016/j.mito.2024.101947.

[3] J. Gong, S. Jiang, Y. Huang, et al., Astaxanthin suppresses the metastasis of clear cell renal cell carcinoma through ROS scavenging, Journal of Functional Foods. 116 (2024) 106139. https://doi.org/10.1016/j.jff.2024.106139.

[4] Z. Ren, H. Yang, C. Zhu, et al., Dietary phytochemicals: As a potential natural source for treatment of Alzheimer's Disease, Food Innovation and Advances. 2 (2023) 36-43. https://doi.org/10.48130/FIA-2023-0007.

[5] Z. Hou, L. Sun, Z. Jiang, et al., Neuropharmacological insights into Gardenia jasminoides Ellis: Harnessing therapeutic potential for central nervous system disorders, Phytomedicine. 125 (2024) 155374. https://doi.org/10.1016/J.PHYMED.2024.155374.

[6] L. Huanhuan, M. Yingying, L. Yanan, et al., Comparative investigation of raw and processed products of Gardeniae Fructus and Gardenia jasminoides var. radicans using HPLC coupled with chemometric methods, Biomedical chromatography : BMC. 35 (2020) e5051. https://doi.org/10.1002/BMC.5051.

[7] W.-W. MA, Y. TAO, Y.-Y. WANG, I.-F. PENG, Effects of Gardenia jasminoides extracts on cognition and innate immune response in an adult Drosophila model of Alzheimer's disease, Chinese Journal of Natural Medicines. 15 (2017) 899-904. https://doi.org/Cnki:Sun:Zgtr.0.2017-12-003.

[8] Y. Nam, D. Lee, Ameliorating effect of Zhizi (Fructus Gardeniae) extract and its glycosides on scopolamine-induced memory impairment, Journal of Traditional Chinese Medicine. 33 (2013) 223-227. https://doi.org/10.1016/S0254-6272(13)60129-6.

[9] W. Xiao, S. Li, S. Wang, C.-T. Ho, Chemistry and bioactivity of Gardenia jasminoides, Journal of Food and Drug Analysis. 25 (2016) 43-61. https://doi.org/10.1016/j.jfda.2016.11.005.

[10] Q. Kankan, Z. Longshan, L. Xinyi, et al., An LC-MS method for simultaneous determination of five iridoids from Zhi-zi-chi Decoction in rat brain microdialysates and tissue homogenates: towards an in depth study for its antidepressive activity, Journal of chromatography. B, Analytical technologies in the biomedical and life sciences. 965 (2014) 206-215. https://doi.org/10.1016/j.jchromb.2014.03.032.

[11] F.-Y. Yuan, C. Ju, C.-X. Zang, et al., Gardenia jasminoides Extract GJ-4 Alleviates Memory Deficiency of Vascular Dementia in Rats through PERK-Mediated Endoplasmic Reticulum Stress Pathway, The American Journal of Chinese Medicine. 51 (2023) 53-72. https://doi.org/10.1142/s0192415x23500040.

[12] L. Lei, Y. Wang, Z. Huo, et al., Variations of Chemical Constituents in Gardeniae Fructus Before and After Stir-frying by LCMS-IT-TOF, Chinese Journal of Experimental Traditional Medical Formulae. 25 (2019) 88-97. https://doi.org/10.13422/j.cnki.syfjx.20190751.

[13] K.-D. Li, Q.-S. Wang, W.-W. Zhang, et al., Gardenia fructus antidepressant formula for depression in diabetes patients: A systematic review and meta-analysis, Complementary Therapies in Medicine. 48 (2020) 102248. https://doi.org/10.1016/j.ctim.2019.102248.

[14] H. Yun-Jung, Y. Ki-Sook, Anti-inflammatory activities of crocetin derivatives from processed Gardenia jasminoides, Archives of pharmacal research. 36 (2013) 933-940. https://doi.org/10.1007/s12272-013-0128-0.

[15] Y.-D. Zhang, M.-H. Wang, M. Guan, et al., Critical Review for active iridoids in Gardenia jasminoides J.Ellis as a plant of food and medicine homology, Food & Medicine Homology. 2 (2025) https://doi.org/10.26599/fmh.2025.9420030.

[16] W. He, Y. Gao, F. Yuan, et al., Optimization of Supercritical Carbon Dioxide Extraction of Gardenia Fruit Oil and the Analysis of Functional Components, JAOCS, Journal of the American Oil Chemists' Society. 87 (2010) 1071-1079. https://doi.org/10.1007/s11746-010-1592-z.

[17] C. Jin, L. Wang, X. Liu, et al., Health oil preparation from gardenia seeds by aqueous enzymatic extraction combined with puffing pre-treatment and its properties analysis, Food Science and Biotechnology. 32 (2023) 2043-2055. https://doi.org/10.1007/s10068-023-01319-9.

[18] D. Wang, A. Bao, Y. Yuan, et al., Whey protein isolate-stabilized gardenia fruit oil nanoemulsions: Ultrasonic preparation, characterization and applications in nutraceuticals delivery, Industrial Crops & Products. 212 (2024) 118345. https://doi.org/10.1016/j.indcrop.2024.118345.

[19] Z. Zhu, G. Luo, F. Zhang, et al., Protective effect of gardenia oil on acute immunologic liver injury induced by ConA in mice, China Oils and Fats. 44 (2019) 99-103. https://doi.org/CNKI:SUN:ZYZZ.0.2019-02-023.

[20] B. Li, Y. Zhang, B. Shi, et al., Gardenia oil increases estradiol levels and bone material density by a mechanism associated with upregulation of COX-2 expression in an ovariectomized rat model, Experimental and therapeutic medicine. 6 (2013) 562-566. https://doi.org/10.3892/etm.2013.1168.

[21] J.R.L.L.X.S.B.X.Q. Fu, Anti-depressant effects of oil from fructus gardeniae via PKA-CREB-BDNF signaling, Bioscience reports. 39 (2019) BSR20190141. https://doi.org/10.1042/bsr20190141.

[22] B. Li, Y. Chen, X. Yang, et al., Extraction technology of gardenia oil and its effect on central nerve system, Journal of the Fourth Military Medical University. 29 (2008) 2152-2155. https://doi.org/CNKI:SUN:DSJY.0.2008-23-021.

[23] W. Tao, H. Zhang, W. Xue, et al., Optimization of Supercritical Fluid Extraction of Oil from the Fruit of Gardenia jasminoides and Its Antidepressant Activity, Molecules. 19 (2014) 19350-19360. https://doi.org/10.3390/molecules191219350.

[24] Q. Ni, Q. Gao, Z. Xu, et al., Analysis of Main Economic Characters of Two Kinds of Gardenia Jasminoides and Components of Their Nut Oil, Journal of the Chinese Cereals and Oils Association. 32 (2017) 78-84. https://doi.org/CNKI:SUN:ZLYX.0.2017-10-015.

[25] Q. Ni, G. Xu, Q. Gao, et al., Evaluation of reactive oxygen species scavenging activities and DNA damage prevention effect of Pleioblastus kongosanensis f. aureostriatus leaf extract by chemiluminescence assay, Journal of Photochemistry & Photobiology, B: Biology. 128 (2013) 115-121. https://doi.org/10.1016/j.jphotobiol.2013.07.018.

[26] A. Zhang, Y. Shen, M. Cen, et al., Polysaccharide and crocin contents, and antioxidant activity of saffron from different origins, Industrial Crops & Products. 133 (2019) 111-117. https://doi.org/10.1016/j.indcrop.2019.03.009.

[27] M.C. Bergonzi, C. Righeschi, B. Isacchi, A.R. Bilia, Identification and quantification of constituents of Gardenia jasminoides Ellis (Zhizi) by HPLC-DAD–ESI–MS, Food Chemistry. 134 (2012) 1199-1204. https://doi.org/10.1016/j.foodchem.2012.02.157.

[28] W. Brand-Williams, M.E. Cuvelier, C. Berset, Use of a free radical method to evaluate antioxidant activity, LWT - Food Science and Technology. 28 (1995) 25-30. https://doi.org/https://doi.org/10.1016/S0023-6438(95)80008-5.

[29] C.C. Guimarães, D.D. Oliveira, M. Valdevite, et al., The glycosylated flavonoids vitexin, isovitexin, and quercetrin isolated from Serjania erecta Radlk (Sapindaceae) leaves protect PC12 cells against amyloid-β25-35 peptide-induced toxicity, Food and Chemical Toxicology. 86 (2015) 88-94. https://doi.org/https://doi.org/10.1016/j.fct.2015.09.002.

[30] T. Mosmann, Rapid colorimetric assay for cellular growth and survival: Application to proliferation and cytotoxicity assays, Journal of Immunological Methods. 65 (1983) 55-63. https://doi.org/https://doi.org/10.1016/0022-1759(83)90303-4.

[31] X. Liu, L. Yao, X. Ye, et al., Danggui-Shaoyao-San (DSS) ameliorating cognitive impairment in ischemia-reperfusion vascular dementia mice through miR-124 regulating PI3K/Akt signaling pathway, Brain research. 1845 (2024) 149135. https://doi.org/10.1016/j.brainres.2024.149135.

[32] Y. Kong, X. Liang, L. Liu, et al., High Throughput Sequencing Identifies MicroRNAs Mediating α-Synuclein Toxicity by Targeting Neuroactive-Ligand Receptor Interaction Pathway in Early Stage of Drosophila Parkinson's Disease Model, PLoS ONE. 10 (2017) e0137432. https://doi.org/10.1371/journal.pone.0137432.

[33] Y.-G. Li, X.-Y. Wang, H.-F. Chen, et al., Comparison of the chemical constituents of raw Fructus Aurantii and Fructus Aurantii stir-baked with bran, and the biological effects of auraptene, Journal of Ethnopharmacology. 269 (2021) 113721. https://doi.org/https://doi.org/10.1016/j.jep.2020.113721.

[34] M.Y. Lee, M. Kim, Effects of Red ginseng on neuroinflammation in neurodegenerative diseases, Journal of Ginseng Research. 48 (2024) 20-30. https://doi.org/https://doi.org/10.1016/j.jgr.2023.08.003.

[35] O.T. O., E.B. E., A.O. B., et al., Gallic acid and neurodegenerative diseases, Phytomedicine Plus. 3 (2023) 100492. https://doi.org/10.1016/j.phyplu.2023.100492.

[36] R. Yao, An in-silico assessment suggests the potential effects of goji (fruit of Lycium barbarum L.) against aging-related diseases, Food & Medicine Homology. 2 (2025) https://doi.org/10.26599/fmh.2025.9420036.

[37] S.H. Alavizadeh, H. Hosseinzadeh, Bioactivity assessment and toxicity of crocin: A comprehensive review, Food and Chemical Toxicology. 64 (2014) 65-80. https://doi.org/https://doi.org/10.1016/j.fct.2013.11.016.

[38] T. Dogan, B.A. Yıldırım, K.A.T. Kapakin, Investigation of the effects of crocin on inflammation, oxidative stress, apoptosis, NF-κB, TLR-4 and Nrf-2/HO-1 pathways in gentamicin-induced nephrotoxicity in rats, Environmental toxicology and pharmacology. 106 (2024) 104374. https://doi.org/10.1016/j.etap.2024.104374.

[39] F.-W. Dong, Z.-K. Wu, L. Yang, et al., Iridoids and sesquiterpenoids of Valeriana stenoptera and their effects on NGF-induced neurite outgrowth in PC12 cells, Phytochemistry. 118 (2015) 51-60. https://doi.org/10.1016/j.phytochem.2015.08.015.

[40] Z.L. El Idrissi, Y. Elouafy, H. El Moudden, et al., Investigation of roasting and photo-oxidative stability of cold-pressed peanut oil: Lipid composition, quality characteristics, and antioxidant capacity, Food Bioscience. 55 (2023) 103046. https://doi.org/https://doi.org/10.1016/j.fbio.2023.103046.

[41] J. Rodríguez-Morató, L. Xicota, M. Fitó, et al., Potential Role of Olive Oil Phenolic Compounds in the Prevention of Neurodegenerative Diseases, Molecules. 20 (2015) 4655-4680. https://doi.org/10.3390/molecules20034655.

[42] D. Yang, S. Zhang, D. Wang, et al., Positive Effects of Seabuckthorn oil on Scopolamine Induced PC12 Cell Damage and APP/PS1 Mice, Natural Product Communications. 20 (2025) https://doi.org/10.1177/1934578x251329127.

[43] Y. Liu, H. Xia, S. Guo, et al., Effect and mechanism of edible oil co-digestion on the bioaccessibility and bioavailability of ursolic acid, Food Chemistry. 423 (2023) 136220. https://doi.org/https://doi.org/10.1016/j.foodchem.2023.136220.

[44] X. Yan, J. Huang, L. Huang, et al., Effects of dietary lipids on bioaccessibility and bioavailability of natural carotenoids, LWT. 200 (2024) 116171. https://doi.org/https://doi.org/10.1016/j.lwt.2024.116171.

[45] J.L. Sonnenburg, F. Bäckhed, Diet–microbiota interactions as moderators of human metabolism, Nature. 535 (2016) 56-64. https://doi.org/10.1038/nature18846.

[46] B. Annett, B. Michael, Bacterial species involved in the conversion of dietary flavonoids in the human gut, Gut microbes. 7 (2016) 216-234. https://doi.org/10.1080/19490976.2016.1158395.

[47] M. Lauss, A. Kriegner, K. Vierlinger, C. Noehammer, Characterization of the Drugged Human Genome, Pharmacogenomics. 8 (2007) 1063-1073. https://doi.org/10.2217/14622416.8.8.1063.

[48] H. Gao, Y. Tao, Q. He, et al., Functional enrichment analysis of three Alzheimer's disease genome-wide association studies identities DAB1 as a novel candidate liability/protective gene, Biochemical and Biophysical Research Communications. 463 (2015) 490-495. https://doi.org/https://doi.org/10.1016/j.bbrc.2015.05.044.

[49] B.S. K, C. Zu-Lin, N.E. H, et al., Blood-derived plasminogen drives brain inflammation and plaque deposition in a mouse model of Alzheimer's disease, Proceedings of the National Academy of Sciences of the United States of America. 115 (2018) E9687-E9696. https://doi.org/10.1073/pnas.1811172115.

[50] P.L. O, V.J. P, M.L. A, S.L. P, CROSS-TALK BETWEEN THE PLASMINOGEN/PLASMIN SYSTEM AND INFLAMMATION RESOLUTION, Journal of thrombosis and haemostasis : JTH. 21 (2023) 2666-2678. https://doi.org/10.1016/j.Jtha.2023.07.013.

[51] D. Majid, R. Niloufar, N. Kulmira, A. Vasso, The Role of Tryptophan Metabolites in Neuropsychiatric Disorders, International Journal of Molecular Sciences. 23 (2022) 9968. https://doi.org/10.3390/ijms23179968.

[52] H. Anna, B. Ewa, K. Wojciech, D.W. Anna, The Engagement of Cytochrome P450 Enzymes in Tryptophan Metabolism, Metabolites. 13 (2023) https://doi.org/10.3390/metabo13050629.

[53] C.A. Salomé, V. Nuno, Tryptophan Metabolism in Depression: A Narrative Review with a Focus on Serotonin and Kynurenine Pathways, International Journal of Molecular Sciences. 23 (2022) 8493. https://doi.org/10.3390/ijms23158493.

[54] T.J. Xia, S.W. Jin, Y.G. Liu, et al., Shen Yuan extract exerts a hypnotic effect via the tryptophan/5-hydroxytryptamine/melatonin pathway in mice, Journal of ethnopharmacology. 326 (2024) 117992. https://doi.org/10.1016/j.Jep.2024.117992.

[55] N. Aktary, Y. Jeong, S. Oh, et al., Unveiling the therapeutic potential of natural products in Alzheimer's disease: insights from in vitro, in vivo, and clinical studies, Frontiers in Pharmacology. 16 (2025) 1601712. https://doi.org/10.3389/fphar.2025.1601712.

[56] Z. Li, C. Gong, NLRP3 inflammasome in Alzheimer's disease: molecular mechanisms and emerging therapies, Frontiers in Immunology. 16 (2025) 1583886. https://doi.org/10.3389/fimmu.2025.1583886.

[57] X. Wang, G. Sun, T. Feng, et al., Sodium oligomannate therapeutically remodels gut microbiota and suppresses gut bacterial amino acids-shaped neuroinflammation to inhibit Alzheimer's disease progression, Cell Research. 29 (2019) 787-803. https://doi.org/10.1038/s41422-019-0216-x.

[58] W. Min, A.W. Kwame, G. Congcong, et al., Effect of oral and intraperitoneal administration of walnut-derived pentapeptide PW5 on cognitive impairments in APPSWE/PS1ΔE9 mice, Free Radical Biology and Medicine. (2022) https://doi.org/10.1016/j.Freeradbiomed.2022.01.003.

[59] Y.H. Jiang, Y.Y. Li, W.G. Xin, et al., Lactiplantibacillus plantarum DACNJS22 alleviates benzo(a)pyrene-induced neurobehavioral injury in mice: Insights from gut microbiota and short-chain fatty acids, Food Bioscience. 64 (2025) 105865. https://doi.org/10.1016/j.Fbio.2025.105865.

[60] V. Marius, K. André, P.D. H, Colonic Butyrate-Producing Communities in Humans: an Overview Using Omics Data, mSystems. 2 (2017) e00130-00117. https://doi.org/10.1128/mSystems.00130-17.

[61] C.M. Elisa, R. Laurie, H.N. T, et al., Inhibition of inflammatory microglia by dietary fiber and short-chain fatty acids, Scientific reports. 13 (2023) 2819. https://doi.org/10.1038/s41598-022-27086-x.

[62] W.H. Oldendorf, Carrier-mediated blood-brain barrier transport of short-chain monocarboxylic organic acids, American Journal of Physiology-Legacy Content. 224 (1973) 1450-1453. https://doi.org/10.1152/ajplegacy.1973.224.6.1450.

[63] P. Zhang, S. Meng, X. Li, J. Liu, Detection of iridoid compounds from Gardenia jasminoides after passing through the blood-brain barrier in dogs, China Pharmacy. 22 (2011) 4419-4421. https://kns.cnki.net/kcms2/article/abstract?v=Jq6vDUSEISAEUo14mMB0uIYbAOOJ10X8KJaMLHZA27wfMR_CLY79i9HXIf2I5qDNGH_8s-GW5qJ6jfyhiGrxZNrTTSWvQ-3fJJtzLQJDfuwqFvY2fSNMaMjfOtF-E-ltAXwsvlf5fsWbes9NoSOICY_M2PtsmtA7L68EX_ZO8JEXLRoIiV7C5A==&uniplatform=NZKPT&language=CHS

[64] M. Lautenschläger, J. Sendker, S. Hüwel, et al., Intestinal formation of trans-crocetin from saffron extract (Crocus sativus L.) and in vitro permeation through intestinal and blood brain barrier, Phytomedicine. 22 (2015) 36-44. https://doi.org/10.1016/j.phymed.2014.10.009.

[65] V. Braniste, M. Al-Asmakh, C. Kowal, et al., The gut microbiota influences blood-brain barrier permeability in mice, Science Translational Medicine. 6 (2014) 263ra158-263ra158. https://doi.org/10.1126/scitranslmed.3009759.

[66] B.J. A, F. Paul, C.M. V, et al., Ingestion of Lactobacillus strain regulates emotional behavior and central GABA receptor expression in a mouse via the vagus nerve, Proceedings of the National Academy of Sciences of the United States of America. 108 (2011) 16050-16055. https://doi.org/10.1073/pnas.1102999108.